A Tunable Loading of Single-Stranded DNA on Gold Nanorods through the Displacement of Polyvinylpyrrolidone

Idah C. Pekcevik[‡], Lester C. H. Poon[‡], Michael C. P. Wang and Byron D. Gates[*]

Department of Chemistry and 4D LABS, Simon Fraser University, 8888 University Drive, Burnaby, British Columbia, V5A1S6 Canada. E-mail: bgates@sfu.ca

KEYWORDS single-stranded DNA, self-assembled monolayers, gold nanorods, polyvinylpyrrolidone, surfactant exchange, surface coverage

ABSTRACT A quantitative and tunable loading of single-stranded (ss-DNA) molecules onto gold nanorods was achieved through a new method of surfactant exchange. This new method involves the exchange of cetyltrimethylammonium bromide surfactants for an intermediate stabilizing layer of polyvinylpyrrolidone and sodium dodecylsulfate. The intermediate layer of surfactants on the anisotropic gold particles was easily displaced by thiolated ss-DNA, forming a tunable density of single-stranded DNA molecules on the surfaces of the gold nanorods. The success of this ligand exchange process was monitored in part through the combination of extinction, X-ray photoelectron and infrared absorption spectroscopies. The number of ss-DNA molecules per nanorod for nanorods with a high density of ss-DNA molecules was quantified through a combination of fluorescence measurements and elemental analysis, and the functionality of the nanorods capped with dense monolayers of DNA was assessed using a

hybridization assay. Core-satellite assemblies were successfully prepared from spherical particles containing a probe DNA molecule and a nanorod core capped with complementary ss-DNA molecules. The methods demonstrated herein for quantitatively fine tuning and maximizing, or otherwise optimizing, the loading of ss-DNA in monolayers on gold nanorods could be a useful methodology for decorating gold nanoparticles with multiple types of biofunctional molecules.

INTRODUCTION

Gold nanoparticles decorated with DNA could be useful for a number of applications, such as biological sensing,[1-4] gene therapy,[5,6] and drug delivery.[7,8] These DNA-nanoparticle conjugates can also serve as building blocks in the formation of self-assembled nanostructures.[9-11] Density of the DNA and other biofunctional molecules coating gold nanoparticles could influence their colloidal stability and their utility in these and other applications. For example, coupling the tunable optical properties of gold nanoparticles[12-14] with the photothermal effect,[15-18] is a simple method of releasing either thiolated DNA[15] or its complementary DNA strand[16-19] from these nanoparticles for gene therapy. The number of DNA molecules attached to the nanoparticles will determine either the corresponding concentration of molecules that can be released as a result of the photothermal activation, or the number of functional groups that can be attached to the surfaces of the gold nanorods. We present a new approach to optimize the loading of thiol-functionalized single-stranded DNA (ss-DNA) monolayers onto gold nanorods in order to fine tune (and maximize) the number of DNA molecules capping these particles.

One of the most widely pursued syntheses of gold nanorods relies on the use of cetyltrimethylammonium bromide (CTAB) surfactants.[13,20-22] These seed mediated syntheses produce gold nanorods capped with a bilayer of CTAB surfactants. Complete displacement of the CTAB bilayer by ss-DNA can be hindered as the CTAB bilayer impedes the formation of the

sulfur-gold bond between the thiolated DNA and the gold nanorod. These molecules can non-specifically interact through electrostatic forces between the positively charged ammonium of CTAB and the negatively charged phosphate backbone of the DNA to create non-uniform multi-layered DNA-CTAB coatings. It is essential to avoid these unwanted interactions in order to achieve reliable and well-packed self-assembled monolayers (SAMs) of ss-DNA on the surfaces of these gold nanorods.

There are a number of methods that have been developed to displace CTAB from the surfaces of gold nanorods, or to otherwise control the electrostatic interactions between CTAB and DNA. One approach is to harness the electrostatic interactions between DNA and positively charged surfaces through the layer-by-layer deposition of polyelectrolytes onto the CTAB coated gold nanorods.[12,23-25] A second approach is through the encapsulation of the nanorods with a thin film of silica.[26] The outer surfaces of this sol-gel derived silica layer are further modified to bind amine- or thiol-functionalized DNA.[27] In a third approach, ss-DNA is decorated onto the gold nanorods through a process of ligand exchange.[15,16,28-30] In this approach, the CTAB bilayers are initially replaced with a short chain alkanethiol (e.g., dodecanethiol). This short thiol-functionalized molecule forms SAMs on the nanorods that are subsequently replaced by ss-DNA through a ligand exchange process.[15,16,29,30] In each of these techniques, the packing density of DNA relies on the ability to uniformly control electrostatic interactions in multilayered films, or to uniformly functionalize a layer of silica, or to completely displace alkanethiol-based SAMs (stabilized by van der Waals interactions) with thiolated ss-DNA. We sought an alternative method to affix a high density of ss-DNA onto the surfaces of gold nanorods.

We have developed a modified approach to decorating the surfaces of the gold nanorods with ss-DNA SAMs by introducing a new intermediate step. This new step replaces the CTAB

stabilizing layer on the gold nanorods with a water-soluble mixture of small molecules (sodium dodecylsulfate, or SDS) and polymers (polyvinylpyrrolidone, or PVP) (Scheme 1). This mixture of surfactants stabilize the nanorods by weakly associating with the gold surfaces,[31,32,33] but can be easily displaced with more strongly binding thiol-functionalized molecules.[34] Polyvinylpyrrolidone forms coordinate bonds between the pyrrolidone sub-units and the surfaces of noble metals.[35-42] These interactions form through electron donation from either the nitrogen or oxygen on a pyrrolidone sub-unit to the metal surfaces. The more dominant interaction is between the carbonyl of the PVP and the surfaces of noble metal nanoparticles.[36,41] Gold particles modified with PVP are stable over a range of pH values,[43] which is useful for dispersing these nanoparticles in a range of media for further decoration. After decoration of the gold nanorods with a mixture of PVP and SDS, we demonstrate the exchange of these weakly coordinated surfactants with thiolated ss-DNA molecules.

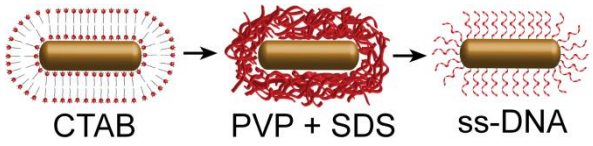

Scheme 1. Schematic representations of as-synthesized gold nanorods capped with cetyltrimethylammonium bromide (CTAB), which is exchanged for a mixture of polyvinylpyrrolidone (PVP) and sodium dodecylsulfate (SDS) as an intermediate step before capping these nanorods with thiol-functionalized single-stranded DNA (ss-DNA).

MATERIALS AND METHODS

***Preparation of PVP and SDS Stabilized Gold Nanorods*:** Gold nanorods were synthesized by a seed-mediated synthesis as discussed in detail in the Supporting Information. The as-

synthesized gold nanorods were purified to remove excess CTAB. This process included centrifugation (Thermo IEC Microlite Microcentrifuge) at 17k rcf for 30 min, followed by decanting the supernatant. The precipitate was subsequently dispersed in 10 mM phosphate buffer at pH 8.0 containing 0.3% w/v SDS. This process of centrifugation, decanting, and suspension of the precipitate in a buffered solution was repeated two more times. A 10 mL aliquot of the purified gold nanorods, suspended in a solution of phosphate buffer and 0.3% SDS, was mixed in a clean round bottom glass flask with a 10 mL solution of PVP (10% w/v in ethanol). The addition of SDS was necessary to prevent aggregation of the purified nanorods and adhesion of these particles to the walls of the centrifuge tubes during the subsequent process of surfactant exchange. This mixture was heated at 40°C with stirring for 18 h. After this period of time, the PVP and SDS modified nanorods were purified by the process described above for centrifugation, decanting and suspension of the precipitate in a solution of phosphate buffer with 0.3% SDS. The concentration of the PVP and SDS stabilized nanorods was determined using the Beer-Lambert law ($\varepsilon = 4.4 \times 10^9$ M^{-1} cm^{-1} at 767 nm) to be 0.32 nM.[44] The extinction spectra for these PVP and SDS modified nanorods had characteristic peaks centered at 513 nm and 760 nm. These nanorods were further modified with the addition of single-stranded DNA that had one end functionalized with a thiol-containing linker.

Preparation of Gold Nanorods Modified with Thiol-Functionalized Single-Stranded DNA (ss-DNA)*:* Solutions of de-protected and purified ss-DNA were added to the PVP and SDS modified gold nanorods (details of the de-protection and purification procedures are included in the Supporting Information). Various concentrations of ss-DNA were prepared by performing serial dilutions of the initial 182 μM ss-DNA with 1×TE buffer to make a total of 8 different samples. The samples were prepared to have a final concentration ratio of thiol-DNA-Quasar to

gold nanorods ranging from 250 to 40,000. Briefly, 10 μL of ss-DNA solution in a 1×TE buffer was added to 200 μL of 0.23 nM gold nanorods modified with PVP and SDS suspended in 10 mM phosphate buffer (pH 8.0) with 0.3% SDS. These mixtures of gold nanorods and ss-DNA were sonicated (Branson Ultrasonic Cleaner, Model 1510) for 5 s and left at room temperature for 16 h before the addition of salt. A salt shielding strategy was used to assist in maximizing the loading of ss-DNA on to the gold nanorods.[45] Briefly, 20 μL of a salting solution—containing 10 mM phosphate (pH 8.0), 300 mM NaCl, 4 mM $MgCl_2$ and 0.3% SDS—was added in a dropwise manner to the mixture of the nanorods and ss-DNA. After addition of the salting solution, the mixtures were sonicated for 5 s. This salting procedure was repeated every 30 min for a total of 10 separate additions of salting solution to achieve a final salt concentration of 10 mM phosphate (pH 8.0), 150 mM NaCl, 2 mM $MgCl_2$ and 0.3% SDS. The salted samples were left at room temperature for a total of 16 h before subsequent purification.

Samples were purified of excess ss-DNA by a series of successive steps that included centrifugation, supernatant removal and suspension of the purified nanorods in a fresh phosphate buffered solution. The samples were centrifuged at 9.3k rcf (Eppendorf 4515 D) for 30 min while held at 4°C. The supernatant was removed and the ss-DNA-nanorod pellet suspended with 200 μL of 10 mM phosphate buffer (pH 8.0) containing 0.3% SDS. The ss-DNA decorated nanorods were suspended into this solution with the aid of 10 s to 1 min of sonication. This purification process was repeated an additional 3 times for a total of 4 supernatant removal steps. Four repetitions of this purification process were sufficient to remove all detectable traces of unbound oligonucleotides from the supernatant (Figure S10). The extinction spectra for these ss-DNA modified gold nanorods had two characteristic LSPR peaks centered at 510 nm and 767 nm. Decanted solutions from this purification process were analyzed for the presence of Quasar

670 by fluorescence spectroscopy. These wash solutions were excited at 644 nm and emission detected at 670 nm with a Cary Eclipse Fluorometer.

The number of ss-DNA decorating the gold nanorods was quantified by treating these samples (measured out in 40 μL aliquots) with 10 μL of 500 mM DTT to achieve a final concentration of 100 mM DTT. The DTT treated samples were left at room temperature for 16 h. After this period of time, both the DTT treated and untreated (control) samples were heated at 90°C for 30 min. All samples were centrifuged at 9.3k rcf (Eppendorf 4515 D) for 30 min while held at 4°C. The supernatant of all samples were removed for subsequent analysis. For the untreated samples, 4 μL of 500 mM DTT was added to 36 μL of the supernatant. The fluorescence of all the treated and untreated samples, negative controls (supporting information), standards (supporting information), and blank solutions [prepared from 10 mM phosphate buffer (pH 8.0) with 0.3% SDS and 100 mM DTT] were measured using a fluorescence microplate reader (Molecular Devices Spectra Max M5) operating at an excitation wavelength of 600 nm while monitoring emission at 670 nm. An excitation wavelength of 600 nm was chosen (as opposed to 644 nm) in order to easily decouple the excitation from the detected emission because the detector was in line with the excitation source within the plate reader. A single standard of Quasar 670 at a concentration of 100 μM was used as a reference to relate the fluorescence readings between each 384 well plate.

RESULTS AND DISCUSSION

The process of exchanging surfactants and forming SAMs of ss-DNA on the gold nanorods was initially monitored by changes in localized surface plasmon resonance (LSPR). The extinction spectra of gold nanorods suspended in phosphate buffer display a shift in the LSPR

associated with each exchange of the dielectric coating. The CTAB coated nanorods had two LSPR peaks centered at 514 nm and 775 nm (Figure 1) that shifted to 512 and 753 nm, respectively, after stabilizing the nanorods with PVP and SDS. Intensity of the LSPR bands also decreased slightly, corresponding to a minimal loss of gold nanorods during this surfactant exchange process. The observed spectral blue shift after this surfactant exchange is attributed to the increased water permeability and decreased thickness of the dielectric coating on the nanorods,[46] which was supported by dynamic light scattering measurements. Subsequent decoration of the nanorods with ss-DNA SAMs resulted in a red-shift of the longitudinal LSPR to 761 nm (Figure 1), confirming a further change in the surface chemistry and a possible increase in the thickness of the dielectric coating. An absorption shoulder at ~665 nm indicates the presence of Quasar 670 labeled ss-DNA attached to the gold nanorods (Figure S1). These spectral shifts suggest changes have taken place in the surface chemistry on the particles, but complementary measurements were required to determine the nature of these changes.

Stable colloidal suspensions are achieved after each surfactant exchange. Changes to the dielectric coating of these colloidal particles were monitored to assess the success of exchanging the surfactants from CTAB to PVP/SDS to ss-DNA. The as-synthesized gold nanorods had a surface potential of +46 mV as determined by zeta potential measurements (Table 1). This zeta potential value is consistent with other reports for CTAB stabilized gold nanorods.[47]

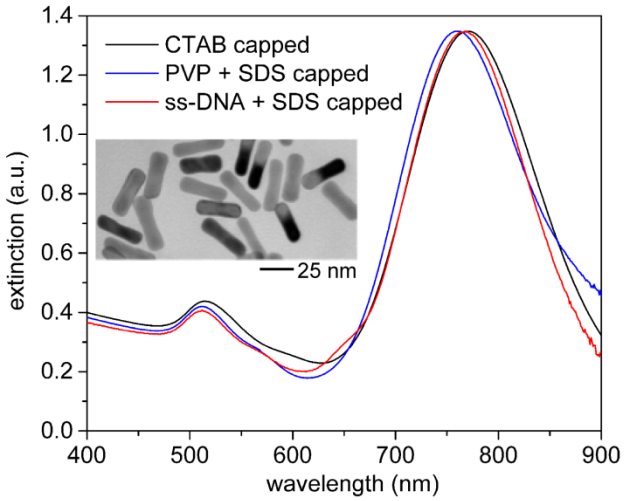

Figure 1. Extinction spectra of solutions containing CTAB (black), PVP and SDS (blue), or ss-DNA (red) capped gold nanorods. The CTAB modified gold nanorods were suspended in water, while both the PVP and SDS modified and the ss-DNA modified gold nanorods were suspended in 10 mM phosphate buffered solution (pH 8.0) containing 0.3% SDS. The inset is a representative transmission electron microscopy (TEM) image of ss-DNA modified gold nanorods.

Replacement of CTAB with a mixture of PVP and SDS shifted the surface potential to –57 mV. A negative surface potential (–50 mV) is also observed after decoration of the nanorods with ss-DNA. The negative surface potentials are attributed to the surfactants adsorbed onto or bound to the surfaces of the gold nanorods (i.e. PVP/SDS and SDS/ss-DNA, respectively).[35,36,42] Changes to the dielectric coating of the nanorods during the surfactant exchange process were also determined by monitoring changes in the average particle size. Average dimensions of the nanorods were monitored by dynamic light scattering (DLS) techniques (Table 1) and transmission electron microscopy (TEM) measurements (Figure S2). Differences in the lengths of the nanorods determined from the DLS and TEM measurements suggested a change in the

thickness of the dielectric coating of the nanorods with each subsequent replacement of the surfactants. The average thickness of the dielectric layer for the CTAB capped nanorods after purification was ~1.5 nm, which is consistent with other literature.[48] Exchange of the CTAB layer for a mixture of PVP and SDS decreased the average thickness of the dielectric coating to ~0.5 nm, which correlates with the observed shift in LSPR mentioned above. Average thickness of the dielectric coating increased to ~3 nm after decorating the nanorods with ss-DNA. This increased thickness of the capping layer is attributed to the formation of 14-mer ss-DNA SAMs on the surfaces of the particles. The thickness of this capping layer is slightly less than the estimated length of the fully extended ss-DNA strand (~4.5 nm). It is most likely that the thickness of the ss-DNA capping layer is less than this theoretical thickness due to the flexibility of the ss-DNA and limitations in accurately determining thickness of the dielectric layer coating on the curved surfaces of the particles.[49] Another possibility is that the dielectric coating on the nanorods is non-uniform due to an incomplete surfactant exchange. The extent of the surfactant exchange was further assessed through a series of spectroscopic measurements.

Completeness of the surfactant exchange process at each step was also monitored by infrared (IR) spectroscopy and x-ray photoelectron spectroscopy (XPS). Infrared spectroscopy confirmed the association of PVP with the nanorods during the intermediate step of this process to cap the nanorods with ss-DNA. Polyvinylpyrrolidone has a strong absorption band centered at 1666 cm^{-1} due to a ν(C=O) stretching vibration.[35,36]

gold nanorods (or AuNRs)	L_h (nm)	T_{dl} (nm)	zeta potential (mV)
AuNRs + CTAB in water	41 ± 3	~1.5	+46 ± 19
AuNRs + PVP in phosphate buffer with SDS	40 ± 3	~0.5	–57 ± 23
AuNRs + ss-DNA in phosphate buffer with SDS	47 ± 5	~3	–50 ± 26

Table 1. Mean hydrodynamic length (L_h), estimated dielectric layer thickness (T_{dl}), and mean zeta potentials determined by dynamic light scattering techniques for gold nanorods (AuNRs) modified with CTAB, PVP and SDS, or ss-DNA and SDS.

This absorption band shifts to 1660 cm^{-1} for the PVP coated nanorods, which is attributed to the coordination of the carbonyl to the gold surfaces.[35,40] Infrared spectroscopy on the DNA decorated nanorods was inconclusive, which was attributed to the structural similarities of PVP and ss-DNA. Analysis by XPS confirmed the presence of gold and silver in the nanorods and the exchange of the capping layers that stabilize these nanoparticles (Figure 2). Bromide ions in the CTAB sample are exchanged for chloride ions associated with sodium salts in the buffer solution used to disperse the PVP and ss-DNA capped particles. The relatively high ratio of C_{1s} to Au_{4f} in the CTAB sample relative to that observed in the other samples is attributed excess CTAB in solution. In addition to these differences observed in the XPS of the three different types of samples, significant differences were also observed in the high-resolution XPS spectra (Figure 3). The carbon species expected from the CTAB samples were hydrocarbons (C-C and C-H) and carbon bound to nitrogen (C-N). These species had characteristic binding energies (BEs) of ~285, and ~287 eV, respectively. The signal also includes carbon bound to oxygen (C-OH) in the form of oxidized adventitious carbon.[50] The carbon species anticipated for the PVP stabilized samples included the addition of amide carbon (N-C=O) with a characteristic binding energy of

~288 eV. The ss-DNA stabilized samples included further species associated with nucleobases, nucleosides, and nucleotides, such as carbon bound to nitrogen (C-N and N-C-N), and urea carbon (N-(C=O)-N). These species have characteristic BEs of approximately ~287 and ~289 eV, respectively.[51,52] The large quantity of unbound CTAB and the compositional differences between the three types of samples is further supported from analysis of the high resolution N_{1s} spectrum (Figure 3b). There is a 3.1 eV shift between the N_{1s} peaks associated with the CTAB molecules that are free in solution (i.e. referred to as unbound CTAB) and those in proximity to the surfaces of the gold nanorods (i.e. referred to as bound CTAB). Distinct N_{1s} spectra were observed when comparing the CTAB and PVP stabilized samples in connection with quaternary and tertiary amines, respectively, within these surfactants. High resolution XPS analysis of the N1s spectral region for ss-DNA capped nanorods also indicated the presence of heterocylic amines, primary amines, and amides.[52] The ss-DNA samples contain amines and amides associated with the bases found in DNA, and Quasar 670 (fluorescent label on ss-DNA). The latter sample also contained sulfur with a binding energy of 168.8 eV attributed to the presence of SDS (Figure S3).[53] We were unable to confirm the presence of S_{2p} peaks at either 162.0 or 163.3 eV due to a poor signal-to-noise ratio. These peaks were anticipated to be present in association with the terminal sulfur of the ss-DNA from either the formation of a gold-sulfur bond or the adsorption of thiol onto the surfaces of the nanorods.[54] Insufficient levels of SDS were present in the PVP stabilized samples for detection by XPS (Figure S3), which is attributed to the fact that these samples were extensively purified prior to XPS analysis and that the SDS was primarily used to prevent unwanted adhesion of the nanorods to the centrifuge tubes during purification. In summary, the IR and XPS analyses provide further evidence that the CTAB molecules were successfully displaced during the surfactant exchange process. There is

insufficient evidence from these results to draw a conclusion on the success of decorating the surfaces of the nanorods with ss-DNA including if PVP was still present in the capping layers of the ss-DNA stabilized particles. Separate control experiments were performed by gel electrophoresis and fluorescence spectroscopy to further assess the presence of the ss-DNA on nanorods and to address the potential for residual PVP on these nanorods.

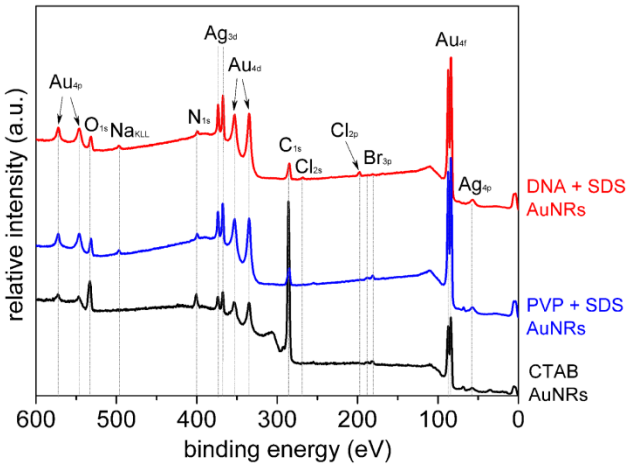

Figure 2. X-ray photoelectron spectra of gold nanorods either capped with CTAB (black line), after exchange with a mixture of PVP and SDS (blue line), or after exchange with a mixture of ss-DNA and SDS (red line).

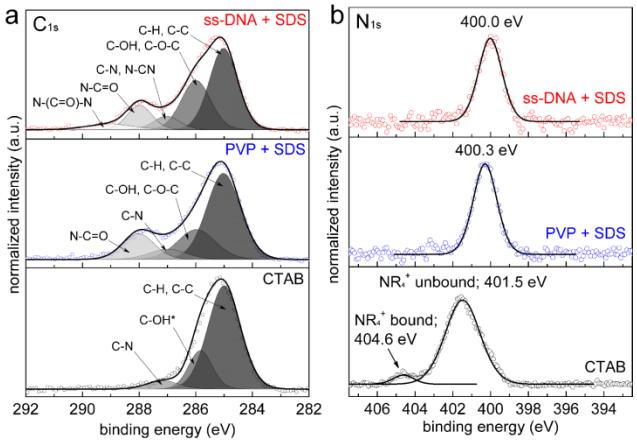

Figure 3. High resolution (a) C_{1s} and (b) N_{1s} XPS spectra of gold nanorods either capped with CTAB, or exchanged for a mixture of PVP and SDS or a mixture of ss-DNA and SDS. Note that C-OH* is most likely an oxidized form of adventitious carbon.[50]

Gel electrophoresis is used to investigate the relative density of charges bound to the surfaces of the gold nanorods. The distance that colloidal particles migrate through a gel under an applied potential is proportional to the number of surface charges and the size of the particles.[29,55] The top row of dark bands in Figure 4a corresponds to the wells in an agarose gel into which the particles were loaded. A solid band is present that spans all the wells corresponding to a blue line drawn below the wells during the preparation of the gels (Figure S4). The red colored bands within the gels below each of the wells indicate the positions of nanorods migrating through each lane in the gel. The red coloration of the nanoparticles corresponds to their surface plasmon resonance properties as observed under white light illumination. This gel electrophoresis of the nanorods indicated that nanorods modified with a mixture of PVP and SDS in phosphate buffer (without additional NaCl and $MgCl_2$) move towards the cathode (Figure 4a, lane 1). A significant difference was observed when comparing the nanorods stabilized with a mixture of PVP and

SDS to those capped with ss-DNA when analyzed by gel electrophoresis under high salt concentrations. The addition of 150 mM NaCl and 2 mM $MgCl_2$ prevented the migration of the PVP and SDS coated nanorods in the gel due to salt induced aggregation (lane 2). In contrast, movement of purified ss-DNA capped nanorods through the gel was not hindered by addition of these salts (lanes 3-10). The distance migrated by a band of nanorods and the concentration of particles within that band (i.e. spatial distribution of particles within a lane) could be related to the number of charge groups (e.g., ss-DNA) bound to the surfaces of the gold particles. This density of thiolated DNA on the nanorods should be proportional to the initial concentration of ss-DNA added to the PVP and SDS stabilized gold nanorods. A series of different particles were prepared by varying the initial ratio of ss-DNA to nanorods (lane 3, particles prepared from an initial ratio of ss-DNA molecules per Au nanorod of 200:1; lane 4, 400:1; lane 5, 800:1; lane 6, 1600:1; lane 7, 3200:1; lane 8, 6400:1; lane 9, 12800:1; lane 10, ~25600:1). Gold particles restricted to the wells or to the start of the lane in the agarose gel (e.g., particles prepared from ratios of ss-DNA to Au nanorod of 200:1) are attributed to a low charge to mass ratio associated with relatively fewer strands of ss-DNA bound to the particles. A further increase in the initial ratio of ss-DNA to nanorods produced diffuse bands of particles in the gel as indicated by the dark streaks in some of the lanes (e.g., lanes 6 to 9). These diffuse bands could be the result of a population of gold nanorods that are non-uniformly coated with ss-DNA. Nanorods that moved more uniformly through the gel, such as the relatively tight single band observed in lane 10 (i.e. particles prepared from a ratio of ss-DNA:Au nanorod of ~25600:1) is, by comparison, attributed to a more dense layer of ss-DNA coating the nanorods. Relative positions of the gold nanorods in each lane of the gel may indicate their colloidal stability and density of surface charges (e.g., ss-

DNA coverage), but further analysis was required to determine the average number of ss-DNA decorating these particles.

The quantity of ss-DNA conjugated through sulfur-gold linkages to each nanorod was determined by fluorescence spectroscopy using Quasar 670 labeled ss-DNA. Briefly, ss-DNA with a Quasar 670 label was released from the surfaces of the purified DNA-gold nanorods by adding dithiothreitol (DTT),[56] and heating the suspension at 90°C for 30 min. Fluorescence emission spectra were collected from the supernatant of the DTT treated samples after removing the gold nanorods by centrifugation (Figure S5b). In addition, a separate experiment was performed to assess the amount of DNA that was potentially non-specifically adsorbed to the DNA-gold nanorod conjugates (e.g., through association with the gold or DNA bound to the surfaces of the nanorods). In this experiment, samples of the DNA-gold nanorod solutions were separately heated at 90°C for 30 min (Figure S5c). Any observed fluorescence from these latter measurements was attributed to non-specifically adsorbed DNA on the nanorods, although these molecules could also be attributed to desorption of thiolated oligonucleotides from the surfaces of the nanorods during their heating. The concentrations of this non-specifically adsorbed DNA (<3% of total fluorescence; see Figure S6) were subtracted from samples treated with DTT and heat in order to remove any potential contribution from DNA bound through non-specific electrostatic interactions when determining the amount of DNA bound to the gold nanorods through sulfur-gold bonds. In order to further evaluate our proposed mechanism of DNA attachment through displacement of PVP and SDS followed by sulfur-gold bond formation, we replaced the thiol functional group with an alcohol functional group on the Quasar 670 labeled DNA. This control investigated the potential interactions between non-thiol-functionalized DNA and the PVP and SDS capped gold nanorods. Fluorescence spectroscopy indicated the absence of

DNA within this sample of particles purified by centrifugation and re-dispersed in 10 mM phosphate buffer in (pH 8.0) with 0.3% SDS (Figure S7). These results suggest that the DNA is not simply intertwined or otherwise strongly interacting with the PVP and SDS, and that the thiol functionality is required for a high loading of DNA onto the surfaces of the gold nanorods.

The number of ss-DNA molecules loaded onto each gold nanorod was proportional to the initial concentration of thiol-functionalized ss-DNA used to form these oligonucleotide-based monolayers and the concentration of gold nanorods in solution. A large excess of ss-DNA was added relative to the number of DNA bound to each nanorod. The concentration of ss-DNA stabilized gold nanorods in solution was determined by inductively coupled plasma mass spectrometry (ICP-MS). The concentration of gold nanorods was further confirmed through calculations using the Beer-Lambert law and an extinction coefficient of 4.4×10^{9} $M^{-1}cm^{-1}$ at 767 nm.[44] These analyses confirmed a concentration of $\sim1.25\times10^{11}$ gold nanorods per mL of solution. The number of thiol-functionalized ss-DNA initially added to each suspension of PVP/SDS stabilized gold nanorods was confirmed by fluorescence spectroscopy, monitoring the Quasar 670 label on each ss-DNA. The number of ss-DNA strands bound to the nanorods was determined after removing excess DNA from the samples followed by DTT treatment and fluorescence spectroscopy (as described above). The results of these spectroscopic measurements were divided by the corresponding concentration of gold nanorods in solution to assess the number of ss-DNA strands bound to each nanorod. The amount of ss-DNA bound to each nanorod steadily increased in proportion to an increase in concentration of thiol-functionalized oligonucleotides added to the nanorods stabilized by a mixture of PVP and SDS (Figure 4b).

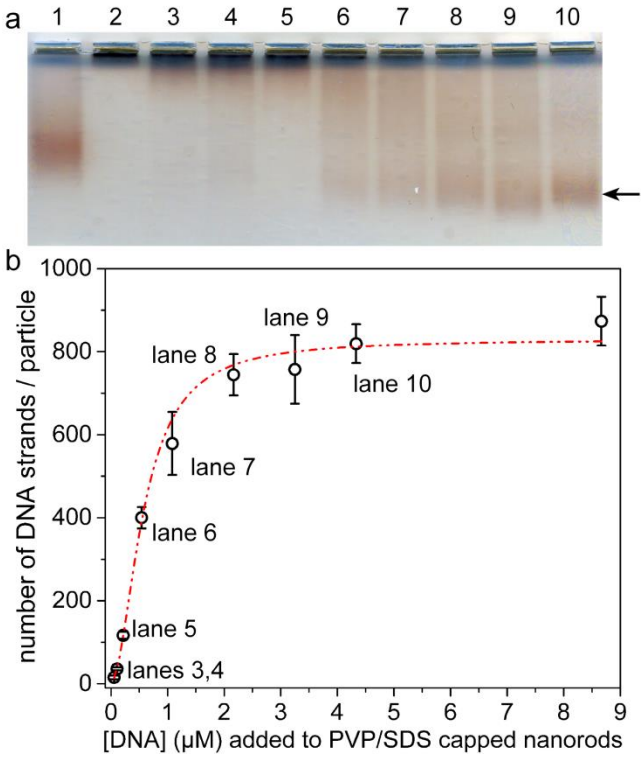

Figure 4. (a) Digital image of an agarose gel after electrophoresis (0.5×TBE buffer and 3% agarose gel) of gold nanorods modified with PVP and SDS (lanes 1 and 2) or modified with various concentrations of ss-DNA (lanes 3 to 10). (b) A plot showing the relationship between the initial concentrations of ss-DNA added to a 0.23 nM solution of PVP/SDS stabilized gold nanorods, and the resulting average number of ss-DNA strands bound to each nanorod in the purified samples. All experiments were run in triplicate and error bars are equivalent to one standard deviation from the mean associated with the variance for these measurements.

The number of ss-DNA molecules bound to each gold nanorod reached a plateau for samples prepared from ratios ≥25600:1 of thiol-functionalized ss-DNA to PVP/SDS stabilized nanorods. This study revealed that the method of displacing the PVP/SDS stabilizing layer with oligonucleotides reached a maximum loading of 870±60 ss-DNA molecules per gold nanorod.

One method to assess the utility of using PVP and SDS as an intermediate stabilizing layer is to compare the surface coverage achieved herein to prior literature. The minimum surface area (or footprint) per ss-DNA molecule was calculated by dividing the total surface area of a nanorod by the maximum loading of ss-DNA molecules. This footprint per ss-DNA molecule is ~2.0 nm^2 for the highest loading achieved in these studies. Previous studies report a footprint of >4 nm^2 per ss-DNA on gold nanorods.[45,57] The density of ss-DNA molecules on the surfaces of the gold nanorods achieved in our studies is close to the maximum loading of ss-DNA achieved on the surfaces of gold films.[49,58,59] In these previous studies, the packing densities of ss-DNA on polycrystalline gold films approached a surface coverage proportional to that of a densely packed monolayer of thiolated oligonucleotides; the effective diameter of the area occupied by each ss-DNA in these studies was between 1.2 and 1.4 nm. The diameter of single-stranded DNA is ~1.2 nm.[49,58] In our studies, the effective diameter of the area occupied by each ss-DNA is estimated to be ~1.5 nm corresponding to a circular footprint with an area of 2.0 nm^2. This improved loading of thiolated ss-DNA on gold nanorods in comparison to the prior literature could be attributed in part to: i) the ease of displacing the PVP and SDS layers relative to displacing other capping molecules (e.g., CTAB, alkanethiol) on the gold nanorods;[60] and ii) the use of multivalent cations (i.e. Mg^{2+}) in solution to stabilize the interactions between the nucleic acids on the gold surfaces.[61,62] The increased density of ss-DNA bound to the gold nanorods in our study could also be due to the differences in the assumed shape of the nanorods used to calculate the surface area (we assumed a dumbbell shape to match the results of our TEM analysis; further details are provided in the Materials and Methods section), as well as the curvature and surface roughness for our gold nanorods prepared in the presence of CTAB in contrast to those prepared by previous studies through electrodeposition.[45,57] A more accurate comparison would require a

detailed, systematic study of nanorods synthesized by the same method and capping layers of ss-DNA assembled under the same conditions, which is beyond the scope of this current study. Our studies demonstrate the ease of exchanging a mixed stabilizing layer of PVP and SDS on gold nanorods with a layer of thiolated ss-DNA. This method avoids potential interference from CTAB molecules through electrostatic interactions that could impede a maximum and uniform loading of ss-DNA onto the gold nanorods.

We also evaluated the ability of the gold nanorods capped with a high loading of ss-DNA to hybridize with complementary probes attached to spherical particles. The success of the hybridization process was evaluated by the ability of these nanorods to form core-satellite assemblies.[9-11] Probe ss-DNA molecules were bound to the surfaces of ~10-nm diameter spherical gold particles. The hybridization process was performed by mixing the spherical and nanorod particles, each decorated with a different ss-DNA molecule that is complementary to each other. The resulting core-satellite assemblies contained an average of 8 spherical particles for every nanorod (Figure 5 and Figure S8). The formation of core-satellite assemblies required the presence of complementary ss-DNA molecules on the nanorods and the nanoparticles (Figure S9).

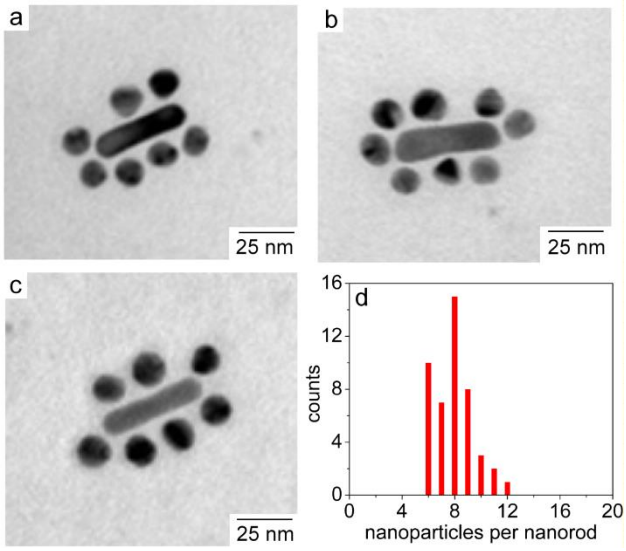

Figure 5. (a-c) Representative TEM images of core-satellite assemblies of gold nanorods decorated with spherical gold nanoparticles. These assemblies form through the hybridization of complementary ss-DNA bound to each type of nanoparticle. (d) A corresponding histogram of satellite particles assembled onto the nanorod cores within a population of ~50 nanorods.

CONCLUSIONS

We have demonstrated a versatile strategy for decorating CTAB capped gold nanorods with oligonucleotides, and demonstrated the ability to fine tune the number of oligonucleotides per nanorod. A mixture of PVP and SDS is used as an intermediate stabilizing layer for the gold nanorods before capping these particles with thiol-functionalized ss-DNA. Analysis by fluorescence spectroscopy demonstrated a reproducible process of decorating the gold nanorods with a well-defined number of oligonucleotides. Colloidal stability of these ss-DNA decorated nanorods in concentrated salt solutions is proportional to the density of oligonucleotides coating their surfaces as assessed by the electrophoretic mobilities of the nanorods. Dense layers of ss-DNA capping the nanorods were prepared with an average footprint down to ~2.0 nm^2. These

particles were used to successfully prepare core-satellite assemblies by a hybridization assay. This new methodology of surfactant exchange could be universally adapted for the uniform and high yielding decoration of gold nanoparticles with other capping groups of interest. The method may also be of use to modify gold nanoparticles with a well-defined number of functional groups in preparation for a variety of applications that include use in drug delivery, photothermal or photodynamic therapies.

ASSOCIATED CONTENT

Supporting Information. Chemical structure of Quasar 670, absorbance spectrum of Quasar 670, extinction spectrum of gold nanorods capped with Quasar modified ss-DNA, TEM images of gold nanorods (CTAB, PVP, and ss-DNA capped) and corresponding histograms for their measured dimensions, high resolution S_{2p} XPS spectra, digital images of an agarose gel after electrophoresis of gold nanorods, calibration curve used to quantify the amount of Quasar modified ss-DNA in solution, fluorescence emission spectra of supernatants collected from the purification of ss-DNA modified gold nanorods, and additional TEM images of nanorod-nanoparticle assemblies and an associated control experiment. "This material is available free of charge via the Internet at http://pubs.acs.org."

AUTHOR INFORMATION

Corresponding Author

* E-mail: bgates@sfu.ca

Author Contributions

‡These authors contributed equally.

Funding Sources

This work was supported in part by the Natural Sciences and Engineering Research Council (NSERC) of Canada, the Canada Research Chairs Program (B.D. Gates), and Community Trust Endowment Funding (CTEF) from Simon Fraser University. This work made use of 4D LABS shared facilities supported by the Canada Foundation for Innovation (CFI), British Columbia Knowledge Development Fund (BCKDF), Western Economic Diversification Canada, and Simon Fraser University.

ACKNOWLEDGMENT

We thank Dr. Dipankar Sen for access to his laboratory and equipment therein.

ABBREVIATIONS

PVP, polyvinylpyrrolidone; SDS, sodium dodecyl sulfate.

REFERENCES

(1) Nam, J. M.; Park, S. J.; Mirkin, C. A. *J. Am. Chem. Soc.* **2002**, *124*, 3820-3821.

(2) Elghanian, R.; Storhoff, J. J.; Mucic, R. C.; Letsinger, R. L.; Mirkin, C. A. *Science* **1997**, *277*, 1078-1081.

(3) Yu, C. X.; Irudayaraj, J. *Anal. Chem.* **2007**, *79*, 572-579.

(4) Cheng, Y. N.; Stakenborg, T.; Van Dorpe, P.; Lagae, L.; Wang, M.; Chen, H. Z.; Borghs, G. *Anal. Chem.* **2011**, *83*, 1307-1314.

(5) Rosi, N. L.; Giljohann, D. A.; Thaxton, C. S.; Lytton-Jean, A. K. R.; Han, M. S.; Mirkin, C. A. *Science* **2006**, *312*, 1027-1030.

(6) Bardhan, R.; Lal, S.; Joshi, A.; Halas, N. J. *Acc. Chem. Res.* **2011**, *44*, 936-946.

(7) Dhar, S.; Daniel, W. L.; Giljohann, D. A.; Mirkin, C. A.; Lippard, S. J. *J. Am. Chem. Soc.* **2009**, *131*, 14652-14653.

(8) Luo, Y. L.; Shiao, Y. S.; Huang, Y. F. *ACS Nano* **2011**, *5*, 7796-7804.

(9) Xu, X. Y.; Rosi, N. L.; Wang, Y. H.; Huo, F. W.; Mirkin, C. A. *J. Am. Chem. Soc*. **2006**, *128*, 9286-9287.

(10) Xu, L. G.; Kuang, H.; Xu, C. L.; Ma, W.; Wang, L. B.; Kotov, N. A. *J. Am. Chem. Soc.* **2012**, *134*, 1699-1709.

(11) Shi, D. W.; Song, C.; Jiang, Q.; Wang, Z. G.; Ding, B. Q. *Chem. Commun.* **2013**, *49*, 2533-2535.

(12) Choi, W. I.; Sahu, A.; Kim, Y. H.; Tae, G. *Ann. of Biomed. Eng.* **2012**, *40*, 534-546.

(13) Ye, X. C.; Jin, L. H.; Caglayan, H.; Chen, J.; Xing, G. Z.; Zheng, C.; Vicky, D. N.; Kang, Y. J.; Engheta, N.; Kagan, C. R.; Murray, C. B. *ACS Nano* **2012**, *6*, 2804-2817.

(14) Alkilany, A. M.; Thompson, L. B.; Boulos, S. P.; Sisco, P. N.; Murphy, C. J. *Adv. Drug Delivery Rev.* **2012**, *64*, 190-199.

(15) Wijaya, A.; Schaffer, S. B.; Pallares, I. G.; Hamad-Schifferli, K. *ACS Nano* **2009**, *3*, 80-86.

(16) Huschka, R.; Zuloaga, J.; Knight, M. W.; Brown, L. V.; Nordlander, P.; Halas, N. J. *J. Am. Chem. Soc.* **2011**, *133*, 12247-12255.

(17) Yamashita, S.; Fukushima, H.; Akiyama, Y.; Niidome, Y.; Mori, T.; Katayama, Y.; Niidome, T. *Bioorg. Med. Chem.* **2011**, *19*, 2130-2135.

(18) Thibaudau, F. *J. Phys. Chem. Lett.* **2012**, *3*, 902-907.

(19) Poon, L.; Zandberg, W.; Hsiao, D.; Erno, Z.; Sen, D.; Gates, B. D.; Branda, N. R. *ACS Nano* **2010**, *4*, 6395-6403.

(20) Nikoobakht, B.; El-Sayed, M. A. *Chem. Mater.* **2003**, *15*, 1957-1962.

(21) Sau, T. K.; Murphy, C. J. *Langmuir* **2004**, *20*, 6414-6420.

(22) Jana, N. R.; Gearheart, L.; Murphy, C. J. *Adv. Mater.* **2001**, *13*, 1389-1393.

(23) Pastoriza-Santos, I.; Pérez-Juste, J.; Liz-Marzán, L. M. *Chem. Mater.* **2006**, *18*, 2465-2467.

(24) Gole, A.; Murphy, C. J. *Chem. Mater.* **2005**, *17*, 1325-1330.

(25) Huang, H. C.; Barua, S.; Kay, D. B.; Rege, K. *ACS Nano* **2009**, *3*, 2941-2952.

(26) Hauck, T. S.; Ghazani, A. A.; Chan, W. C. W. *Small* **2008**, *4*, 153-159.

(27) Sendroiu, I. E.; Warner, M. E.; Corn, R. M. *Langmuir* **2009**, *25*, 11282-11284.

(28) Grabinski, C.; Schaeublin, N.; Wijaya, A.; D'Couto, H.; Baxamusa, S. H.; Hamad-Schifferli, K.; Hussain, S. M. *ACS Nano* **2011**, *5*, 2870-2879.

(29) Wijaya, A.; Hamad-Schifferli, K. *Langmuir* **2008**, *24*, 9966-9969.

(30) Vigderman, L.; Manna, P.; Zubarev, E. R. *Angew. Chem. Int. Ed*. **2012**, *51*, 636-641.

(31) Hou, W. B.; Dehm, N. A.; Scott, R. W. J. *J. Catal.* **2008**, *253*, 22-27.

(32) Pastoriza-Santos, I.; Gomez, D.; Perez-Juste, J.; Liz-Marzan, L. M.; Mulvaney, P. *Phys. Chem. Chem. Phys.* **2004**, *6*, 5056-5060.

(33) Caschera, D.; Federici, F.; Zane, D.; Focanti, F.; Curulli, A.; Padeletti, G. *J. Nanopart.Res.* **2009**, *11*, 1925-1936.

(34) Tsunoyama, H.; Nickut, P.; Negishi, Y.;Al-Shamery, K Matsumoto, Y.; Tsukuda, T. *J. Phys. Chem. C* **2007**, *111*, 4153-4158.

(35) Kan, C. X.; Cai, W. P.; Li, C. C.; Zhang, L. D. *J. Mater. Res.* **2005**, *20*, 320-324.

(36) Kedia, A.; Kumar, P. S. *J. Phys.Chem. C* **2012**, *116*, 23721-23728.

(37) Liu, H.; Zhang, B.; Shi, H. Q.; Tang, Y. J.; Jiao, K.; Fu, X. *J. Mater. Chem.* **2008**, *18*, 2573-2580.

(38) Mdluli, P. S.; Sosibo, N. M.; Revaprasadu, N.; Karamanis, P.; Leszczynski, J. *J. Mol. Struct.* **2009**, *935*, 32-38.

(39) Behera, M.; Ram, S. *Appl. Nanosci*. **2013**, DOI: 10.1007/s13204-013-0198-9.

(40) Seoudi, R.; Fouda, A. A.; Elmenshawy, D. A. *Physica B* **2010**, *405*, 906-911.

(41) Tu, W. X.; Zuo, X. B.; Liu, H. F. *Chin. J. Polym. Sci.* **2008**, *26*, 23-29.

(42) Zhang, J. H.; Liu, H. Y.; Wang, Z. L.; Ming, N. B. *Chem. Eur. J.* **2008**, *14*, 4374-4380.

(43) Lim, D. K.; Cui, M. H.; Nam, J. M. *J. Mater. Chem.* **2011**, *21*, 9467-9470.

(44) Liao, H. W.; Hafner, J. H. *Chem. Mater.* **2005**, *17*, 4636-4641.

(45) Hill, H. D.; Millstone, J. E.; Banholzer, M. J.; Mirkin, C. A. *ACS Nano* **2009**, *3*, 418-424.

(46) Tagliazucchi, M.; Blaber, M. G.; Schatz, G. C.; Weiss, E. A.; Szleifert, I. *ACS Nano* **2012**, *6*, 8397-8406.

(47) Hu, X. G.; Gao, X. H. *Phys. Chem. Chem. Phys.* **2011**, *13*, 10028-10035.

(48) Gómez-Graña, S.; Hubert, F.; Testard, F.; Guerrero-Martínez, A.; Grillo, I.; Liz-Marzán, L. M.; Spalla, O. *Langmuir* **2012**, *28*, 1453-1459.

(49) Steel, A. B.; Levicky, R. L.; Herne, T. M.; Tarlov, M. J. *Biophys. J.* **2000**, *79*, 975-981.

(50) Barr, T. L.; Seal, S. *J. Vac. Sci. Technol. A* **1995**, *13*, 1239-1246.

(51) May, C. J.; Canavan, H. E.; Castner, D. G. *Anal. Chem*. **2004**, *76*, 1114-1122.

(52) Lee, C.-Y.; Gong, P.; Harbers, G. M.; Grainger, D. W.; Castner, D. G.; Gamble, L. J. *Anal. Chem*. **2006**, *78*, 3316-3325.

(53) Terlingen, J. G. A.; Feijen, J.; Hoffman, A. S. *J. Colloid Interface Sci.* **1993**, *155*, 55-65.

(54) Vericat, C.; Vela, M. E.; Benitez, G.; Carro, P.; Salvarezza, R. C. *Chem. Soc. Rev.* **2010**, *39*, 1805-1834.

(55) Kim, J. Y.; Kim, H. B.; Jang, D. J. *Electrophoresis* **2013**, *34*, 911-916.

(56) Hurst, S. J.; Lytton-Jean, A. K. R.; Mirkin, C. A. *Anal. Chem*. **2006**, *78*, 8313-8318.

(57) Cederquist, K. B.; Keating, C. D. *ACS Nano* **2009**, *3*, 256-260.

(58) Rekesh, D.; Lyubchenko, Y.; Shlyakhtenko, L. S.; Lindsay, S. M. *Biophys. J.* **1996**, *71*, 1079-1086.

(59) Song, Y. H.; Liu, Y. Q.; Yang, M. L.; Zhang, B. L.; Li, Z. *Appl. Surf. Sci.* **2006**, *252*, 5693-5699.

(60) Xia, X. H.; Yang, M. X.; Wang, Y. C.; Zheng, Y. Q.; Li, Q. G.; Chen, J. Y.; Xia, Y. N. *ACS Nano* **2012**, *6*, 512-522.

(61) Russell, R.; Millett, I. S.; Doniach, S.; Herschlag, D. *Nat. Struct. Biol.* **2000**, *7*, 367-370.

(62) Fang, X. W.; Littrell, K.; Yang, X.; Henderson, S. J.; Siefert, S.; Thiyagarajan, P.; Pan, T.; Sosnick, T. R. *Biochemistry* **2000**, *39*, 11107-11113.

for TOC Only